Available online at www.sciencedirect.com
ScienceDirect
Ceramics International 35 (2009) 2007–2015
CERAMICS INTERNATIONAL
www.elsevier.com/locate/ceramint

Influence of raw material type and of the overall chemical composition on phase formation and sintered microstructure of mullite aggregates

Ibram Ganesh [a,b], José M.F. Ferreira [b,*]

[a] Center for Advanced Ceramics, International Advanced Research Centre for Powder Metallurgy and New Materials (ARCI), Hyderabad 500005, A.P., India
[b] Department of Ceramics and Glass Engineering, CICECO, University of Aveiro, Aveiro P-3810193, Portugal

Received 16 June 2008; received in revised form 9 September 2008; accepted 7 November 2008
Available online 3 December 2008

Abstract

Dense mullite aggregates with varied (47–70%) alumina contents have been prepared by a conventional dry-powder pressing technique followed by heat treatments at temperatures in the range of 1450–1725 °C. Different types of clays, beach sand sillimanite (BSS) and a high purity aluminium hydroxide were used as starting materials. Mullites derived from BSS consisted of equi-axed grains whereas those obtained from clay containing precursor mixtures exhibited elongated grains. The bulk density (BD), apparent porosity (AP) and water absorption (WA) capacity of sintered mullites were found to be strongly influenced by the pre-mullitization step of the precursors and in a less extent by the type of raw material, its hydration degree and the impurity contents of Fe_2O_3, CaO and Na_2O. Mullite aggregates obtained from the three different types of aluminosilicate raw materials (i.e., ball clay, china clay and beach sand sillimanite) through a double-stage heat treatment process exhibited better sintered properties in terms of bulk density, apparent porosity, water absorption capacity and higher mullite contents in comparison to those obtained following a single-stage firing process.

Keywords: D. Mullite; Ball clay; China clay; Beach sand sillimanite; Double-stage firing process

1. Introduction

Mullite is known for its several important properties such as, good chemical inertness, low thermal conductivity, high creep resistance, high refractoriness and low thermal expansion coefficient [1–5]. For most applications, mullite is synthetically made following various routes, with predominance of reaction sintering from alumina and silica precursors. The stable composition range of mullite in the Al_2O_3–SiO_2 system is ≅70.5–74 wt.% Al_2O_3, and its theoretical density varies between 3160 and 3220 kg/m^3. The stoichiometric mullite $3Al_2O_3{\cdot}2SiO_2$ corresponds to 71.8 wt.% alumina [3]. The performance of refractory materials based on mullite, is governed by chemical composition, which usually contain 47–70 wt.% Al_2O_3 [4], and by the sintered microstructure. Fused mullite or sintered mullite with low grain boundary populations and relatively large size (>40 μm) equi-axed grains are preferred for refractory applications due to their relatively high resistance to attack by the slag [6]. The morphology of mullite grains derived from silica-rich compositions is needle-like, whereas that from alumina-rich compositions is more equi-axed. The evolution of mullite microstructure is not only influenced by the chemical composition but also by the nature of the starting raw materials [7]. In the case of naturally occurring raw materials, sillimanite group of minerals leads to the formation of mullites with equi-axed grains, whereas kaolinite leads to needle-like grains. However, none of the existing mullite-related articles clearly demonstrated the effects of naturally occurring raw materials and chemical composition on the formation, densification behaviour and sintered microstructure [8,9]. Normally, cheap, readily and abundantly available high purity natural raw materials like kaolinite, sillimanite, ball clay, bauxite (gibbsite and diaspore) and halloysite are preferred for the production of refractory grade mullite aggregates [1–9]. The mullite aggregates formed from these raw materials show a falloff in properties such as, high-temperature strength, corrosion resistance and chemical durability, in proportion to impurity levels [10].

* Corresponding author. Tel.: +351 234 370242; fax: +351 234 370204.
E-mail address: jmf@ua.pt (J.M.F. Ferreira).

0272-8842/$34.00
doi:10.1016/j.ceramint.2008.11.008

In this investigation, we have undertaken a systematic study to establish the effects of raw material type and chemical composition on the formation, densification behaviour and sintered microstructure of relatively high purity mullite aggregates formed from abundantly available natural raw materials. For this purpose, mullite-based compositions having 47–70 wt.% alumina were formulated using beach sand sillimanite (BSS), ball clay, china clay and high purity aluminium hydroxide as raw materials. The actual alumina content of stoichiometric mullite varies in the range of 70.5–74 wt.% [3]. The batch formulations were homogenised, compacted by uni-axial dry-powder pressing technique and then heat treated for 1–3 h at temperatures in the range of 1450–1725 °C before and after subjecting to an intermediate calcination treatment at 1250–1300 °C for 1 h. The differently sintered mullites were thoroughly characterized for bulk density (BD), apparent porosity (AP), water absorption (WA) capacity, XRD phase composition and microstructural features in order to understand the relationships between the final properties, the heat treatment schedule, and the characteristics of starting raw materials.

2. Experimental procedure

2.1. Raw materials and powder processing

Commercial ball clay (BC) and china clay (CC) procured from Mysore Minerals Ltd., Bangalore, India, and a beach sand sillimanite (S) from Indian Rare Earth Ltd., Kerala, India, were used as sources of aluminosilicates. A commercial aluminium tri-hydroxide (A) (NALCO, NSPH-10, India) synthesized according to the Bayer process was used as a source of alumina. The physicochemical properties of raw materials as provided by the suppliers are presented in Table 1. For comparison purposes, commercial mullite samples (Mulcoa 47, Mulcoa 60 and Mulcoa 70), procured from M/s. CE Minerals, China, were also used in this study.

In a typical experiment, powder mixtures containing different amounts of alumina and aluminosilicate sources were co-ground for 6 h in a rotary steel jar mill (250 mm diameter and 300 mm height) using steel balls (20 mm diameter) and a balls to charge ratio of 2:1. The ground powders mixtures were converted into granules with sizes <595 μm with the help of an aqueous polyvinyl alcohol (PVA) solution (5 wt.%). Dried granules were pressed uni-axially under 200 MPa pressure into pellets having 30 or 70 mm diameter × 10 mm height. Pressed pellets were then heat treated for 1–3 h in an electrically operated open-air furnace at 1450–1725 °C using a heating rate of 180 °C/h. Some of the raw materials mixtures were subjected to an intermediate calcination process prior to sintering. In this case, ground raw materials mixtures were initially converted into extrudable dough in a Sigma kneader (Frigmayers, India) with the help of 30% aqueous solution containing 3 wt.% dextrin (Loba-Chemie, India) and then extruded into 20 mm diameter rods using a twin-screw horizontal extruder (BB Engineering Works, India). Extrudates were oven dried at 120 °C overnight and calcined for 1 h at 1250–1300 °C under the same conditions reported above to obtain powders with mullite phase contents >60%. All the calcined powders were once again ground for 6 h under the same conditions reported above prior to pressing and final sintering.

2.2. Material characterization

The XRD patterns were recorded on a Bruker (Karlsruhe, Germany) D8 advanced system using diffracted beam monochromated Cu Kα (0.15418 nm) radiation source. Crystalline phases were identified by comparison with Powder Diffraction File (PDF)-4 reference data from International Centre for Diffraction Data (ICDD). Easy Quant, the semi-quantitative feature of JADE software, was used to calculate the weight percent of each identified phase [11,12]. The JADE software uses the peak area information along with the phase RIR (relative intensity ratios). The vitreous phase was disregarded in the XRD analysis because it could not be quantified with the facilities available in our lab. It will be higher in the silica-rich compositions and will enhance the liquid phase diffusion of species, facilitating the earlier formation of mullite and its needle-like morphology. Particle size analysis of powders was determined using a particle size analyzer (Granulometer G 920,

Table 1
Raw materials specifications[a].

Property	Ball clay	China clay	Sillimanite	Aluminium hydroxide
Code given	BC	CC	S	A
Al_2O_3 (wt.%)	34.2	35.16	53.5	64.5
SiO_2 (wt.%)	48.7	49.98	40.1	0.009
ZrO_2 (wt.%)	–	–	2.5	–
CaO (wt.%)	0.28	0.51	0.5	0.03
MgO (wt.%)	0.31	0.22	0.3	–
Fe_2O_3 (wt.%)	1.6	0.65	0.80	0.007
Na_2O (wt.%)	0.21	0.18	0.07	0.23–0.30
K_2O (wt.%)	1.21	0.09	0.2	–
TiO_2 (wt.%)	1.28	1.13	1.3	0.26–0.32
LoI (RT–1000 °C)	12.21	12.08	0.73	34.50
Average particle size (μm)	7.30	5.16	6.32	5.12
Crystalline phases	–	Kaolinite	Sillimanite	γ-Al_2O_3 (>90%); α-Al_2O_3 (<10%)

[a] Provided by the suppliers.

Cilas, France). Bulk density, apparent porosity and water absorption capacity of various sintered mullites were measured according to Archimedes principle (ASTM C372) using Mettler balance and the attachment (AG 245, Mettler Toledo, Switzerland). For this purpose, about 10–15 sintered pellets (∼15 mm diameter and 8 mm height) were randomly selected from each batch and crushed into 3–5 mm sized grains and a ∼20 g of each sample was taken for measuring the sintered properties [13,14]. Three density measurements were performed for each sample to determine the average and the standard deviation values (±0.01 error). Linear shrinkage values underwent by the pellets subjected to different sintering temperatures were determined by dimensional measurements. Microstructures of dense mullite grains were examined by SEM (JSM-5410, JEOL, Japan) with an energy dispersive (EDAX) scanning attachment (Sigma 3.42 Quaser, Kevex, USA). The samples mounted on araldite platforms were polished, chemically etched (phosphoric acid at 185 ± 5 °C for 4 min) and then gold coated for SEM observation. The coefficient of thermal expansion (CTE) of sintered samples was measured with a Netzsch 402C dilatometer in the temperature range of 30–1000 °C.

3. Results and discussion

The commercial mullite samples having 47%, 60% and 70% Al_2O_3 (Mulcoa 47, Mulcoa 60 and Mulcoa 70) with bulk densities of 2600–2620 kg/m^3 [85.6–86.29% of the theoretical density (TD)], 2750–2780 kg/m^3 (84.14–85.06% TD) and 2800–2880 kg/m^3 (81.25–83.57% TD), apparent porosities of 3.6%, 2.8% and 3.5% and mullite phase contents of 65%, 77% and 87%, respectively, have proved their suitability in refractory applications [2]. The main objective of the present study was to produce mullite aggregates from beach sand sillimanite or other relatively abundantly available natural raw materials having similar, or better, properties in comparison to those of the above commercial mullites.

Table 2 presents the raw materials ratio, and data about average particle size and the chemical compositions of precursor mixtures in terms of Al_2O_3, CaO, Fe_2O_3, Na_2O contents, loss on ignition (LoI RT to 1000 °C), green density (GD) of pressed compacts, bulk density, apparent porosity, water absorption capacity and XRD phases of the samples fired for 1 h at 1650 °C (a single-stage firing process). For simplicity reasons, different codes are given to compositions. Numbers 47, 60 and 70 in the sample codes represent the percentages of Al_2O_3. Among the three aluminosilicates (ball clay, china clay and sillimanite), used as starting raw materials, only BC and CC contain >48 wt.% SiO_2 allowing the synthesis of mullites with 47 wt.% Al_2O_3. The data reported in Table 2 show that the most extensive transformation into mullite occurred in less alumina-rich compositions, probably due to the formation of a more abundant liquid phase upon sintering. Though, among the various mullites prepared, only the mullite (M70-ACC, Table 2) with 70% alumina formed from china clay exhibited comparable bulk density and apparent porosity values to that of Mulcoa 70 upon sintering for 1 h at 1650 °C. However, the

Table 2
Properties of different types of mullites processed according to a single-stage reaction sintering process at 1650 °C for 1 h[a].

Sample[b]	Raw materials (wt. ratio)	CaO (wt.%)	Fe_2O_3 (wt.%)	Na_2O (wt.%)	LoI[c] (wt.%)	APS (μm)	GD (kg/m^3)	BD (kg/m^3)	TD[d] (kg/m^3)	RD (%)	AP (%)	WA (%)	XRD phases (%)			
													M	A	T	C
M47-ACC	A:CC, 15.53:84.46	0.434	0.549	0.186	12.66	4.85	1970	2480	3036	81.68	1.41	0.58	70.91	26.06	1.38	1.65
M47-ABC	A:BC, 12.2:87.77	0.248	1.403	0.220	14.73	5.12	1990	2350	3036	77.40	1.33	0.57	66.7	21.25	2.45	9.54
M60-AS	A:S, 9.3:90.6	0.455	0.725	0.091	3.389	5.32	2070	2480	3268	75.88	1.0	0.41	76.4	21.2	0.43	0.2
M60-ACC	A:CC, 38.16:61.83	0.326	0.789	0.410	19.50	4.88	1960	2650	3268	81.09	3.13	1.18	78.94	20.79	0.27	0.00
M60-ABC	A:BC, 37.59:62.40	0.185	1.0	0.243	20.42	4.92	2330	2580	3268	78.94	0.17	0.06	72.83	21.97	3.08	2.12
M70-AS	A:S, 38.3:61.6	0.319	0.495	0.158	13.33	5.43	2200	2660	3446	77.19	18.18	6.83	86.21	9.12	0.78	1.43
M70-ACC	A:CC, 55.79:44.20	0.241	0.290	0.246	23.76	4.84	2210	2810	3446	81.54	1.55	0.70	24.06	74.12	0.36	1.46
M70-ABC	A:BC, 44.81:55.18	0.141	0.719	0.259	24.38	4.31	2310	2690	3446	78.06	6.44	2.39	47.43	50.82	0	1.75

[a] Properties determined as described in Section 2; APS, average particle size; GD, green density; BD, bulk density; TD, theoretical density; RD, relative density; AP, apparent porosity; WA, water absorption capacity; XRD, X-ray diffraction; M, mullite; A, corundum; T, trydimite; C, cristobalite (vitreous phases were not considered in the quantitative estimation of XRD phases).
[b] The numbers 47, 60 and 70 in the sample codes denote the targeted alumina contents in the samples.
[c] Between RT and 1000 °C.
[d] Obtained based on rule of mixture of Al_2O_3 (3980 kg/m^3) and SiO_2 (2200 kg/m^3) densities.

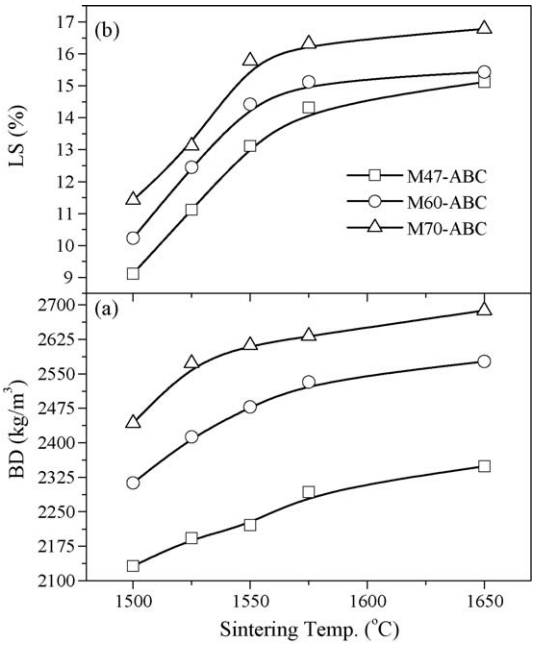

Fig. 1. Bulk density (BD) (a) and linear shrinkage (LS) (b) of M47-ABC, M60-ABC and M70-ABC compacts heat treated at different temperatures.

amount of mullite phase formed is very less (only about 24%) in comparison to Mulcoa 70 which had 87% mullite phase.

To understand the evolution of mullite phase and the densification behaviour upon firing, the compacts of M47-ABC, M60-ABC and M70-ABC formulated from relatively abundant (in south India) ball clay and high purity alumina hydroxide powder were heat treated for 1 h at 1500, 1525, 1550, 1575 and 1650 °C (in a single-stage firing process using a heating rate of 180 °C/h). The measured values of bulk density and the associated linear shrinkage (LS) of these samples are plotted in Fig. 1a and b, respectively. It can be seen that the evolution of all BD and LS curves with temperature increasing is similar for all compositions, showing a faster increasing step up to about 1550 °C, followed by a more gradual increase for higher temperatures. This slowing in densification and shrinkage rates can be attributed to hindering effect caused by the increasing amounts of low density mullite phase that are preferentially formed within the higher heat treatment temperature range. But the BD and LS values are higher for the alumina-richer compositions due to the higher density of Al_2O_3 (3980 kg/m^3). Accordingly, as the heat treatment temperature increased from 1500 to 1650 °C, the BD and LS values of M47-ABC increased from 2132 to 2350 kg/m^3 and from 9.12% to 15.12%, respectively; while the increments for M60-ABC and M70-ABC were from 2313 to 2580 kg/m^3 and 10.23% to 15.43% and from 2443 to 2690 kg/m^3 and 11.42% to 16.78%, respectively. The expected more abundant liquid phase formed in silica-richer compositions, facilitating the earlier formation of mullite also activates the hindering densification effect due to the associated volume expansion [15–18]. This drawback can be minimised by using a double-stage firing process intermediated by grinding/homogenisation and re-compaction steps that shorten the diffusion paths, enhancing the mullite formation and densification processes.

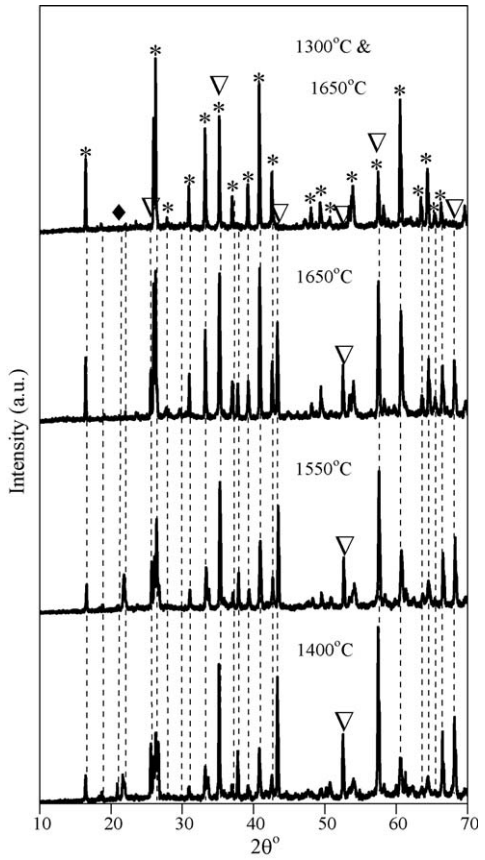

Fig. 2. XRD patterns of M70-ABC compacts heat treated at different temperatures for 1 h [*, lines are due to mullite ($3Al_2O_3{\cdot}2SiO_2$, File No.: 00-015-0776); ▽, due to corundum (α-Al_2O_3, File No.: 00-046-1212); ◆, due to cristobalite (SiO_2, File No.: 01-071-6245)].

Fig. 2 compares the XRD patterns of the M70-ABC composition heat treated for 1 h at 1400, 1550 and 1650 °C (single-stage firing process) and at 1650 °C for the same time period but after being initially heat treated for 1 h at 1300 °C followed by grinding/homogenisation and re-compaction (double-stage firing process). It can be seen that the samples submitted to single-stage firing process exhibit diffraction lines due to mullite, corundum and cristobalite phases, whereas the double-stage firing process resulted in diffraction lines only due solely to mullite phase. Corundum and cristobalite are the major phases in the samples heat treated at 1400 and 1550 °C. The sample treated at 1650 °C exhibits mullite as major phase, but considerable amounts of corundum and cristobalite phases are still present.

The SEM micrographs of M70-ABC heat treated for 1 h at 1400, 1550 and 1650 °C (single-stage firing process) are presented in Fig. 3. It can be seen that the amount of needle-like grains increases with temperature increasing, being consistent with the increased intensity of the XRD mullite peaks results (Fig. 2). This mullite morphology is very common when starting from clay minerals, being enhanced if a liquid phase develops during sintering [18] as can be expected in the presence of some impurities (CaO, Fe_2O_3 and Na_2O). These

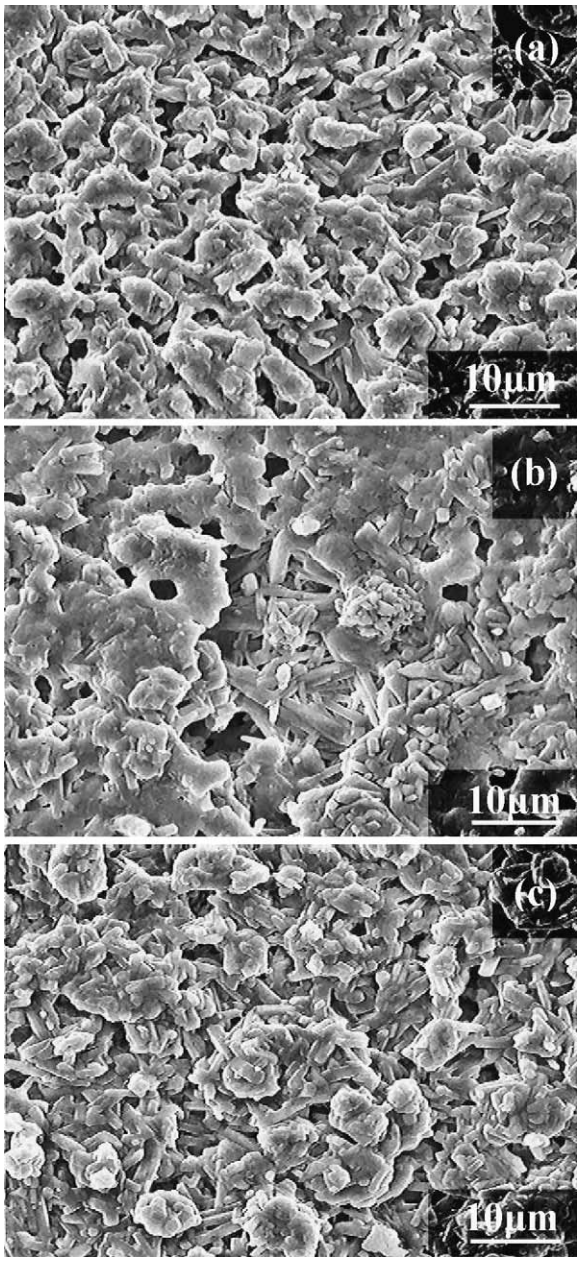

Fig. 3. SEM micrographs of M70-ABC mullite aggregates sintered for 1 h at (a) 1400 °C, (b) 1550 °C and (c) 1650 °C (single-stage firing process).

impurities and the hydration degree of the raw materials might also affect the formation and densification behaviour of mullites. None of the samples submitted to single-stage firing (1 h at 1650 °C) cumulatively satisfied the commercial criteria in terms of sintered properties. CaO and Na_2O are effective mineralizers even at low concentrations (<1%) [15]. Among the three impurities, Fe_2O_3 present in considerable amounts (i.e., up to 1.3%), did not show any significant effect either on densification behaviour or mullite phase formation, probably due to the solid-solution forming capability of mullite towards Fe_2O_3, which can incorporate up to 10–12 wt.% of Fe_2O_3 at temperatures >1300 °C [16]. Therefore, iron oxide may not be available for acting as mineralizer or grain growth inhibitor [16].

However, the desired mullite phase contents and bulk density values could hardly be obtained using single-stage firing process. The main reasons are the relatively large average particle size (∼5 μm) of precursor mixtures (Table 2) and the volume expansion associated with the mullite phase formation [1–5].

The volume expansion associated with the formation of low density crystalline phases is a problem common to the synthesis of other commercially important refractory ceramics, like $MgAl_2O_4$ spinel grains from Al_2O_3 and MgO. To overcome this problem, a double-stage firing process was employed to obtain dense stoichiometric $MgAl_2O_4$ [13,14]. Spinel phase contents up to about 80% were initially obtained by subjecting the raw materials mixtures to an intermediate calcination (1400 °C) step, followed by grinding, compaction and sintering at 1650 °C. However, in the case of mullite, the influence of intermediate calcination step on the densification behaviour and mullite formation has not been studied so far.

In order to study the influence of an intermediate calcination step, the precursor mixtures designed to produce mullites with 70% Al_2O_3 (i.e., M70-AS, M70-ACC and M70-ABC in Table 2) were first calcined for 1 h at 1250–1300 °C followed by re-grinding, compaction and a second-stage heat treatment for 1–3 h at temperatures in the range of 1550–1650 °C. The precursor mixture, M70-AS, was calcined for 1 h at 1250 °C and sintered for 1 h at 1550 °C, whereas the precursor mixtures, M70-ACC and M70-ABC, were calcined for 1 h at 1300 °C and sintered for 1 h at 1650 °C. The values of average particle size of precursor mixtures, GD of pressed compact, BD, AP, WA capacity and the mullite phase contents of samples after double-stage firing are given in Table 3. It can be seen that all the as heat treated samples exhibit sintered properties comparable to those of commercial Mulcoa 70 aggregates, but higher mullite contents. In the case of sillimanite-based precursor mixture, the required sintered properties were achieved even after sintering for 1 h at 1550 °C. This lowering of the sintering temperature anticipates important energy savings.

The evolution of properties (BD, AP and WA capacity) of mullites derived from the M47-ABC, M60-ABC and M70-ABC compositions single fired at 1650 °C (1–3 h) and submitted to double-stage firing (1 h at 1300 °C, re-ground to fine powders, compacting and sintering at 1650 °C (1–3 h) is presented in Fig. 4. It can be seen that in general, the M70-ABC exhibits superior sintered properties as compared to M47-ABC and M60-ABC. Further, the increase in soaking time from 1 to 3 h has slightly improved the degree of densification of single-stage heat treated samples. The decrease of AP and WA with increasing soaking time is more evident for the sample M60-ABC. However, BD did not achieve a value comparable to that of commercial products [2]. An increase of BD from 2950 to 3070 kg/m^3 was reported for a stoichiometric 3:2 mullite upon sintering at 1600 °C with soaking time increasing from 2 to 10 h [3]. These results suggest that longer soaking times (∼10 h, instead of 3 h) will be required for promoting enough densification and phase transformation in a single-stage firing process. However, such long soaking times are difficult to maintain in industrial production, particularly when using

Table 3
Properties of different types of mullites processed according to a double-stage reaction firing process and sintered for 1 h at 1550 and 1650 °C[a].

Sample[b]	APS (μm)	GD (kg/m^3)	BD (kg/m^3)	RD (%)	AP (%)	WA (%)	XRD phases (%)			
							M	A	T	C
M70-ACC-1650	4.93	2170	2890	83.86	0.4	0.6	90.2	2.1	0.6	5.3
M70-ABC-1650	5.03	2220	2910	84.44	0.9	0.5	96.3	0	0	3.2
M70-AS-1550	5.10	2180	2950	85.60	0.2	0.3	100	–	–	–

[a] Properties determined as described in Section 2. 1550 and 1650 denote the second-stage heat treatment temperature. The first-stage heat treatment temperature was at 1250 °C/1 h for precursor mixture M70-AS, and at 1300 °C/1 h for precursor mixtures M70-ACC and M70-ABC. APS, average particle size; GD, green density; BD, bulk density; RD, relative density; AP, apparent porosity; WA, water absorption capacity; XRD, X-ray diffraction; M, mullite; A, corundum; T, trydimite; C, cristobalite (vitreous phases were not considered in the quantitative estimation of XRD phases).
[b] The number 70 in the sample codes denotes the targeted alumina contents in the samples.

rotary kilns. Interestingly, the mullites prepared *via* double-stage firing process revealed the desired sintered properties, which can be ranked in the following order: M70-ABC > M60-ABC > M47-ABC.

Fig. 5 shows the XRD patterns of the M47-ABC, M60-ABC and M70-ABC samples prepared *via* double-stage firing process. Only mullite phase could be identified in the M70-ABC, while small bumps (encircled) in the range of 20–30° 2θ and an increased background noise observed in the patterns of M47-ABC and M60-ABC samples indicating the presence of a glassy phase. The single-stage fired (1650 °C, 1 h) samples M47-ABC, M60-ABC and M70-ABC revealed mullite phase contents of 66.7%, 76.13% and 47.43%, respectively (along with varying amounts of corundum, cristobalite and tridymite – Table 2), which are lower than those reported by Skoog and Moore [3], probably due to differences in chemical compositions of the starting raw materials and average particle sizes. Interestingly, these precursor mixtures gave mullite aggregates with properties comparable to those of commercial products *via* a double-stage firing process. These results are in good agreement with THE other literature reports [3]. It has been also reported that, for clay containing mullite precursor mixtures, the rate of mullite formation and the required temperature depend on the chemical purity and particle size distribution of raw materials. When kaolinite containing precursor mixtures are heated, kaolinite first converts into meta-kaolinite in the temperature range of 450–600 °C by the process of dehydration. Between 450 and 600 °C, kaolinite crystals undergo the breakdown of their structure with the release of chemically combined water to form meta-kaolinite [17]. At about 950 °C, meta-kaolin transforms into spinel with the ejection of amorphous silica. Small cuboidal crystals of primary mullite begin to develop in the clay relicts at 1000 °C or above. Upon further heating, needle-shaped crystals of secondary mullite,

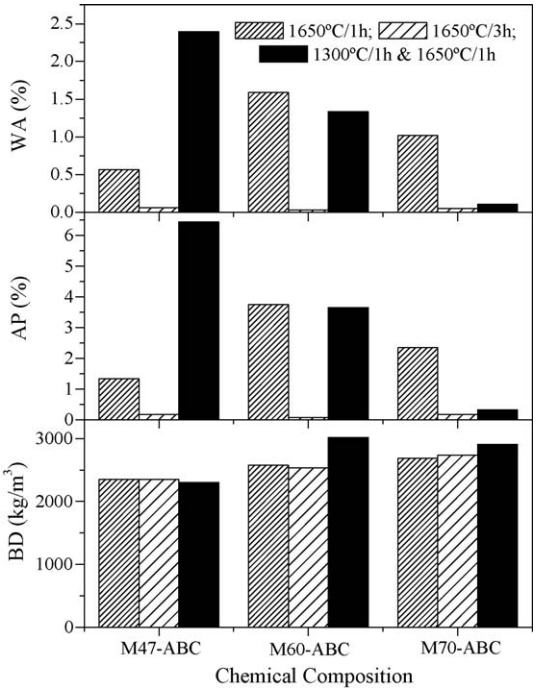

Fig. 4. Evolution of BD, AP and WA of the aggregates M47-ABC, M60-ABC and M70-ABC with sintering temperature (single- and double-stage firing processes).

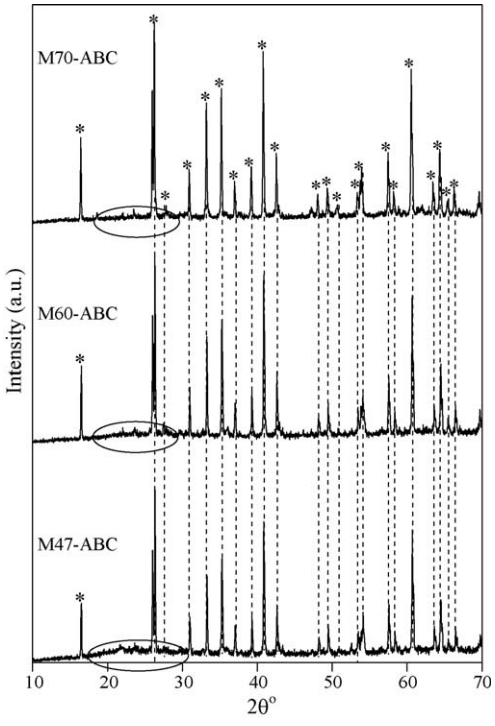

Fig. 5. XRD patterns of the aggregates M47-ABC, M60-ABC and M70-ABC sintered for 1 h at 1650 °C (double-stage firing process). The precursor mixtures were initially calcined for 1 h at 1300 °C, ground, compacted and then sintered [*, lines are due to mullite ($3Al_2O_3{\cdot}2SiO_2$, File No.: 00-015-0776)].

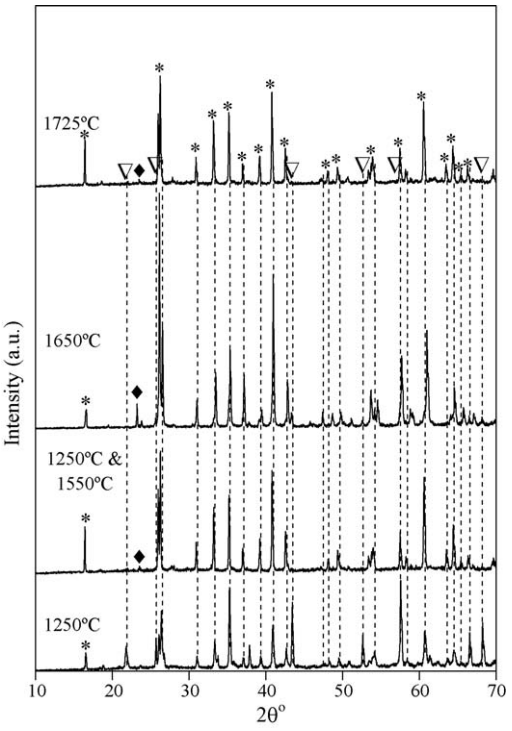

Fig. 6. XRD patterns of M70-AS heat treated at different temperatures [*, lines are due to mullite ($3Al_2O_3{\cdot}2SiO_2$, File No.: 00-015-0776); ▽, due to corundum (α-Al_2O_3, File No.: 00-046-1212); ◆, due to cristobalite (SiO_2, File No.: 01-071-6245)].

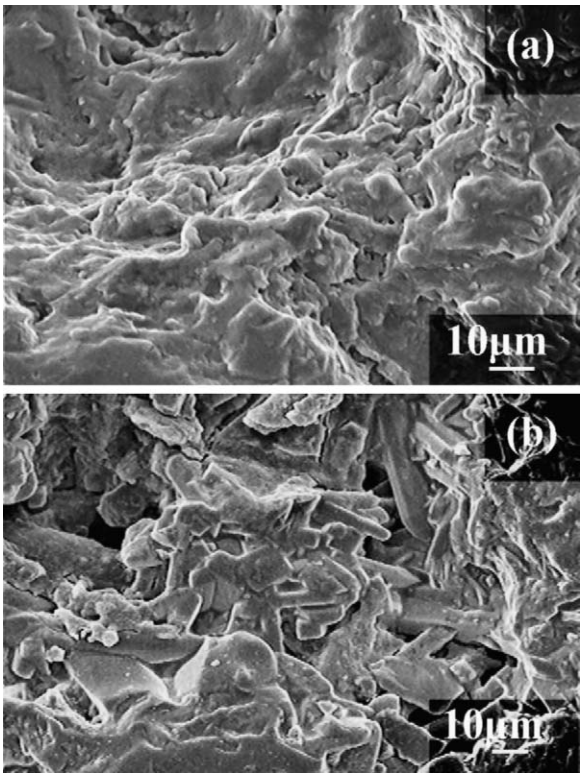

Fig. 7. SEM micrographs of mullite aggregates sintered for 1 h at 1650 °C (double-stage firing process): (a) M60-ABC and (b) M70-ABC. The precursor mixtures were initially calcined for 1 h at 1300 °C, ground, compacted and then sintered.

crystallising from the clay relicts in the presence of a liquid phase [18]. The rate of the secondary mullite formation was reported to be very slow at 1555 °C and extremely fast at 1600 °C due to the strong effect of the eutectic liquid formation at 1595 °C between alumina and silica [3].

The XRD patterns of M70-AS fired under different heat treatment schedules are presented in Fig. 6. The mullite contents formed upon calcination at 1250 °C for 1 h varied in the range of 60–70% along with some minor amounts of cristobalite, tridymite and corundum when 5–6 samples (*ca.* 5 g each) were randomly collected from the 20 kg batch and analyzed by XRD. This calcined powder then transformed into ~100% mullite after sintering for 1 h at 1550 °C. This contrasts with the mullite content of only 86% obtained from the same precursor mixture M70-AS upon single-stage firing for 1 h at 1650 °C (Table 2). This incomplete reaction is certainly due to the long diffusion paths for the reacting species. Earlier investigations have shown that mullite phase formation at relatively lower temperature (<1600 °C) is favoured by using fast heating rates and submicron powders having high surface energy [6,7]. However, there are known difficulties in obtaining submicron size powders by dry milling. The high costs required for wet milling the starting precursor mixtures up to submicron sizes necessary for the production of refractory grade mullite aggregates *via* a single-stage firing process are also well known. Therefore, the use of pre-mullitization step seems to be an alternative processing route for the economic production of dense mullite aggregates from the precursor mixture containing BSS upon sintering 1 h at 1550 °C.

The microstructural features of mullite aggregates derived from precursor mixtures containing ball clay (M60-ABC and M70-ABC) and china clay (M60-ACC and M70-ACC) *via* a double-stage firing process (1300 °C for 1 h + 1650 °C for 1 h), and BSS containing precursor mixtures (M60-AS and M70-AS) *via* a double-stage firing process (1250 °C for 1 h + 1550 °C for 1 h), are presented in Figs. 7–9, respectively. These micrographs show clear morphological differences between the grains formed from different chemical compositions and from different starting raw materials. In general, materials derived from formulations containing clay minerals consist of relatively elongated grains. This is more evident for compositions with 60% Al_2O_3 (Figs. 7a and 8a) in which a more abundant liquid phase is expected to form upon sintering in comparison to materials with 70% Al_2O_3 (Figs. 7b and 8b), although this morphology is still clearly observed for this overall composition in the china clay-derived mullite (Fig. 8b). In contrast, mullites formed from sillimanite-based precursor mixtures (M60-AS and M70-AS) consist of equi-axed grains (Fig. 9). The orthorhombic symmetry and atomic structure tends to favour needle-like habit of mullite [3]. This habit seems to be less dependent on the Al_2O_3:SiO_2 ratio but instead appears to depend more on the presence of other oxides that favour the formation of a glassy phase [3]. The usually encountered association of needle-shaped mullite crystals and a glass phase is the weak link in high-temperature properties and corrosive

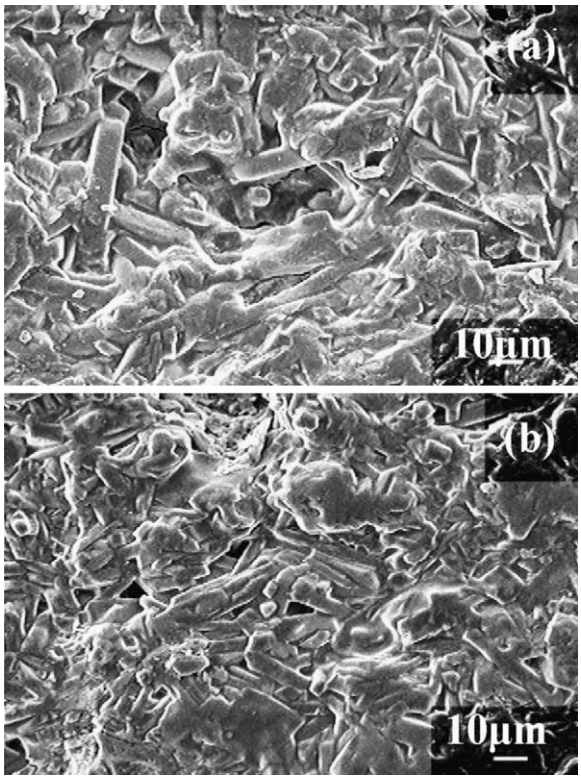

Fig. 8. SEM micrographs of mullite aggregates sintered for 1 h at 1650 °C (double-stage firing process): (a) M60-ACC and (b) M70-ACC. The precursor mixtures were initially calcined for 1 h at 1300 °C, ground, compacted and then sintered.

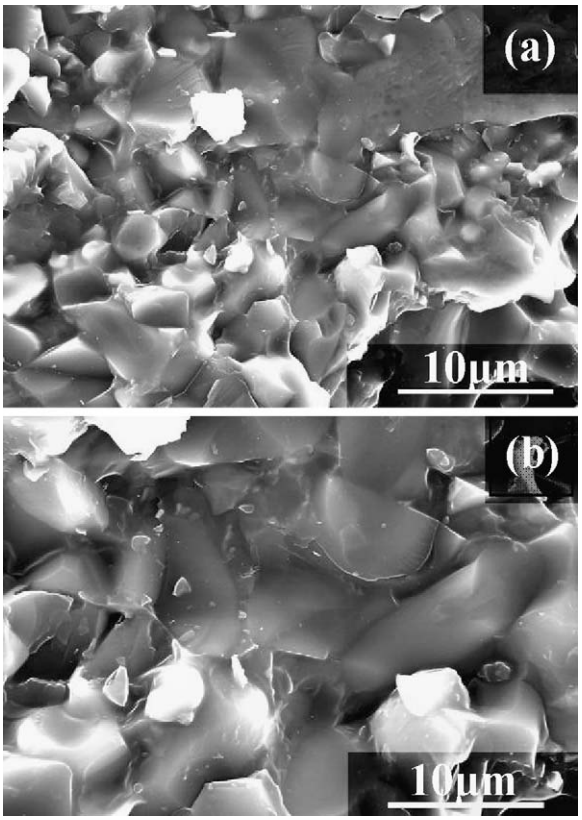

Fig. 9. SEM micrographs of mullite aggregates sintered for 1 h at 1550 °C (double-stage firing process): (a) M60-AS and (b) M70-AS. The precursor mixtures were initially calcined for 1 h at 1250 °C, ground, compacted and then sintered.

environments. It has been reported that a chunky/equi-axed morphology is formed upon sintering mullite in the absence of a liquid phase, whereas the needle-like habit apparently required a liquid phase and a fairly rapid cooling rate [1–9]. All studies show that mullite needles grow preferentially along the *c*-axis [7–9]. These observations can be loosely used as a tool to interpret the mechanism active in mullite formation. Chunky habit is mostly observed in the case of sintered refractories and is indicative of low residual glassy phase. Thus, the mullites derived from M60-AS and especially from M70-AS can be preferentially used for high-temperature refractory applications [1–9].

Mullites derived from BSS containing M60 and M70 compositions *via* a double-stage firing process (1250 °C, 1 h + 1550 °C, 1 h) exhibited CTE values of 4.491×10^{-6} and 4.524×10^{-6} °C^{-1}, respectively, between 30 and 1000 °C. In general, the CTE values of these two samples are comparable with those reported (4.5×10^{-6} and $(4.4–4.6) \times 10^{-6}$ °C^{-1} between 30 and 1000 °C) for high purity mullites [1,2,19,20]. The difference measured between the CTE values of M60 and M70 is very nominal indicating that thermal expansion of M60 and M70 mullites formed from BSS containing precursor mixtures do not depend much on the chemical composition within this range of values. Viswabaskaran et al. [19], noticed a slight decrease in the CTE of mullite when it was doped with 3 wt.% MgO, attributed to the formation of a secondary low CTE cordierite phase. Haldar and Banerjee [21] prepared mullite–40% ZrO_2 composites from beach sand sillimanite by sintering at 1600 °C for 2 h in the presence of 2–8% MgO as sintering aid. They have noticed an increase in the CTE from 4.49×10^{-6} to 6.13×10^{-6} °C^{-1} as magnesia concentration increased from 2.12 to 4.33 wt.% in the mullite–zirconia composite. They have attributed this increase in CTE to the formation of glassy phase having high CTE in the presence of magnesia which caused expansion. The M60 and M70 aggregates derived from BSS contain total amounts of impurities of about 3.5 and 2.5 wt.%, respectively, and exhibited CTE values that are almost coincident with that of high purity stoichiometric mullite [2], being well suited for mullite refractory applications [1,3].

The chemical composition of M70-AS mullite aggregates after double-stage firing as determined by EDAX analysis is

Table 4
Chemical composition of M70-AS mullite as determined by EDAX analysis.

Composition	wt.%
Al_2O_3	67.58
SiO_2	25.47
MgO	1.11
ZrO_2	2.89
CaO	0.28
Na_2O	1.70
Fe_2O_3	0.62
TiO_2	0.25
Cr_2O_3	0.1

reported in Table 4. The results indicate slightly higher concentrations of most of the minor oxides reported in Table 2 (Na_2O, ZrO_2 and Fe_2O_3), and also the presence of other minor oxides such as MgO, TiO_2 and Cr_2O_3, and consequently, slightly lower concentrations of Al_2O_3 and SiO_2 and ZrO_2 in comparison to the target composition. Considering that EDAX is not a very accurate analysis method, it seems reasonable to conclude that the chemical composition of the M70-AS-derived mullite aggregates is well comparable with the target composition and with that of commercial Mulcoa 70 grade mullite [3].

4. Conclusions

The following conclusions can be drawn from the above study:

(1) The mullite ceramics derived from beach sand sillimanite contain equi-axed grains, which are preferred for refractory applications, whereas mullites derived from ball clay and china clay containing precursor mixtures consist of elongated grains, which are known as weak points in high-temperature refractory applications.
(2) Pre-mullitization of precursor mixtures helps in obtaining mullite aggregates with much improved sintered properties even at relatively lower sintering temperatures over mullites formed in the single-stage firing process.
(3) Dense mullite aggregates with sintered properties (BD, AP, WA capacity and XRD phase content) equivalent to, or even better than those revealed by commercial Mulcoa products can be prepared using beach sand sillimanite as a low-cost, readily and abundantly available raw material following a conventional double-stage firing process.

Acknowledgements

I.G. thanks SERC-DST (Government of India) for the awarded BOYSCAST fellowship (SR/BY/E-04/06). The financial support of CICECO is also acknowledged.

References

[1] H. Schneider, J. Schreuer, B. Hildmann, Structure and properties of mullite – a review, J. Eur. Ceram. Soc. 28 (2008) 329–344.
[2] R. Bolger, Fused mullite – niche market material, IM Fused Miner. Rev. (1997), 44–46.
[3] A.J. Skoog, R.E. Moore, Refractory of the past for the future: mullite and its use as a bonding phase, Ceram. Bull. 67 (7) (1988) 1180–1185.
[4] K.S. Mazdiyasni, L.M. Brown, Synthesis and mechanical properties of stoichiometric aluminum silicate (mullite), J. Am. Ceram. Soc. 55 (11) (1972) 548–552.
[5] J.A. Santillan, H.B. Ramirez, R.C. Bradt, Dense mullite from attrition milled kyanite and α-alumina, J. Ceram. Proc. Res. 8 (1) (2007) 1–11.
[6] H.S. Tripati, G. Banerjee, Effect of chemical composition on sintering and properties of Al_2O_3–SiO_2 derived from sillimanite beach sand, Ceram. Int. 25 (1) (1999) 19–25.
[7] H.S. Tripati, S.K. Das, B. Mukherjee, A. Ghosh, G. Banerjee, Synthesis and thermo-mechanical properties of mullite–alumina composite derived from sillimanite beach sand: effect of ZrO_2, Ceram. Int. 27 (8) (2001) 833–837.
[8] G.W. Brindley, M. Nakahira, The kaolinite–mullite reaction series: I, a survey of outstanding problems, J. Am. Ceram. Soc. 42 (7) (1959) 311–314.
[9] J.E. Comeforo, R.B. Fischer, W.F. Bradley, Mullitization of kaolinite, J. Am. Ceram. Soc. 31 (9) (1948) 254–259.
[10] V. Viswabaskaran, F.D. Gnanam, M. Balasubramanian, Mullitisation behaviour of south Indian clays, Ceram. Int. 28 (2002) 557–564.
[11] B.D. Cullity, Elements of XRD, 2nd ed., Addison-Wesley, Reading, MA, 1978.
[12] M.P. Klug, L.E. Alexander, X-ray Diffraction Procedure for Polycrystalline and Amorphous Materials, Wiley, New York, 1974, p. 634.
[13] I. Ganesh, S.M. Olhero, A.H. Rebelo, J.M.F. Ferreira, Formation and densification behavior of magnesium aluminate spinel: the influence of processing parameters, J. Am. Ceram. Soc. 91 (6) (2008) 1905–1911.
[14] I. Ganesh, K.A. Teja, N. Thiyagarajan, R. Johnson, B.M. Reddy, Formation and densification behavior of magnesium aluminate spinel: the influence of CaO and moisture in the precursors, J. Am. Ceram. Soc. 88 (10) (2005) 2752–2761.
[15] P.D.D. Rodrigo, P. Boch, High-purity mullite ceramics by reaction sintering, Int. J. High Technol. Ceram. 1 (1985) 3–30.
[16] R.F. Davis, J.A. Pask, High Temperature Oxides, Academic Press, New York, 1971.
[17] C.J. McConville, W.E. Lee, Microstructural development on firing illite and smectite clays compared with that in kaolinite, J. Am. Ceram. Soc. 88 (8) (2005) 2267–2276.
[18] Y. Iqbal, W.E. Lee, Fired porcelain microstructure revisited, J. Am. Ceram. Soc. 82 (12) (1999) 3584–3590.
[19] V. Viswabaskaran, F.D. Gnanam, M. Balasubramanian, Mullite from clay–reactive alumina for insulating substrate application, Appl. Clay Sci. 25 (2004) 29–35.
[20] K.N. Lee, R.A. Miller, Development and environmental durability of mullite and mullite/YSZ dual layer coatings for SiC and Si_3N_4 ceramics, Surf. Coat. Technol. 86–87 (1996) 142–148.
[21] M.K. Haldar, G. Banerjee, Properties of zirconia–mullite composites from beach sand sillimanite, Mater. Lett. 57 (2003) 3513–3520.